Supplemental Table 6 (Excel file)

List of genes elevated in proteinuric versus non-proteinuric kidneys assessed fo
the comparison between changes induced by G-744, P506-15 or
cyclophosphamide treatment versus vehicle control as summarized in Figure 6(

Supplemental Figures

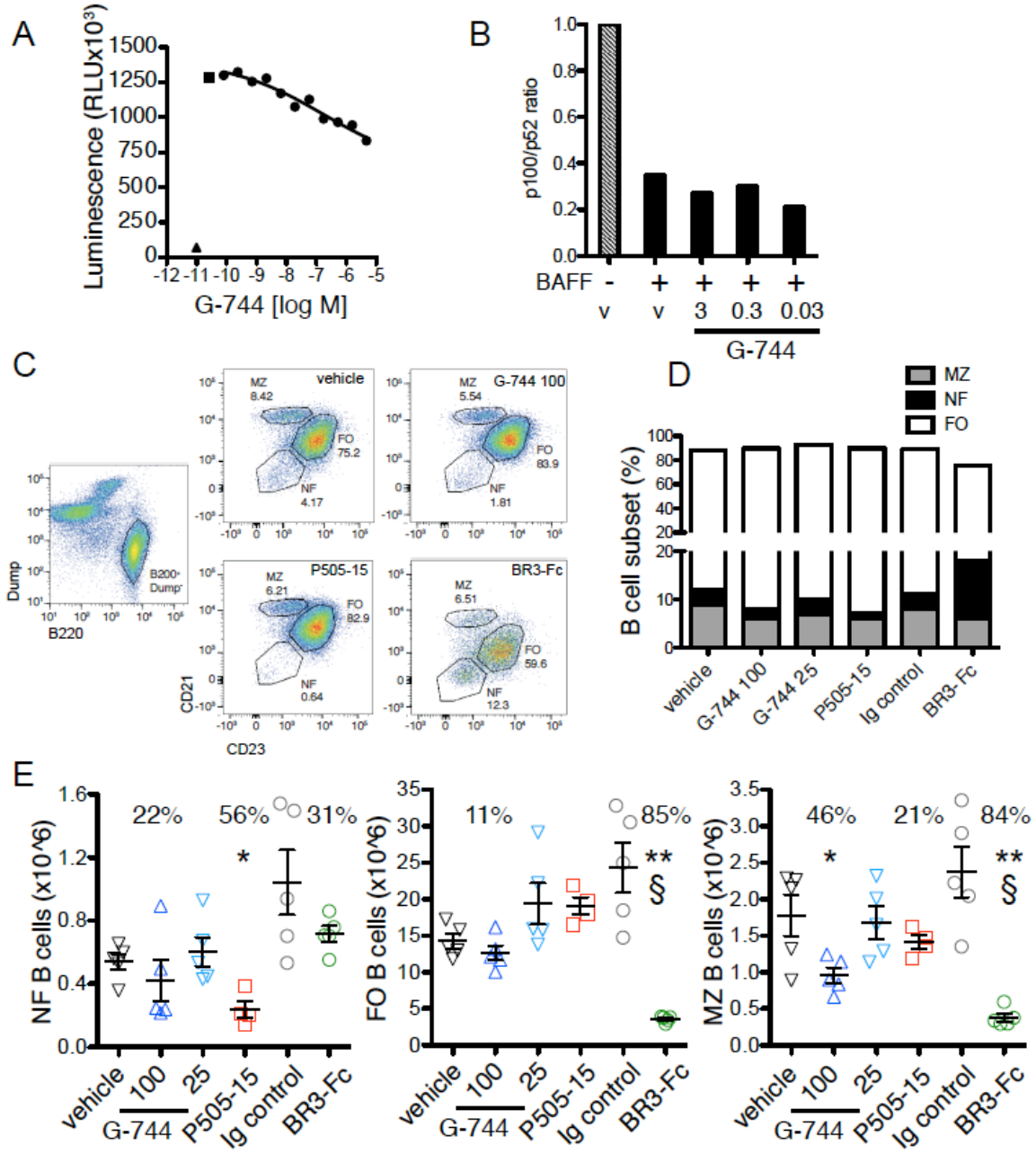

Supplemental Figure 1

Effect of Btk and Syk inhibition on BAFF receptor function and splenic B cells subsets. (**A**) Graph shows mean survival, as measured by CellTiterGlow luminescence, in response to BAFF after 4 days of murine B cells treated with

different concentrations of G-744 or vehicle-treated unstimulated B cells (square) and vehicle treated BAFF-activated B cells (triangle). A representative experiment of 4 experiments is shown. (**B**) Graph of the p100/p52 ratio from splenic B cells that had been cultured with (+) or without (-) BAFF for 16h in the presence of vehicle (v) or different concentration of G-744. Levels of p100 and p52 relative to p38 as loading control were determined by Western blot. The ratio of p100/p52 was normalized to control B cells cultured without BAFF. (**C-E**) Effect of Btk and Syk inhibitor treatment compared to BR3-Fc on splenic B cell populations. C57BL/6 mice were treated BID for 7 days with vehicle, 100mg/kg G-744, 25 mg/kg G-744 or 60mg/kg P505-15, or mice were injected 4x per week with 10mg/kg Ig control or BR3-Fc. B cell subsets were determined by flow cytometry. B cells were gated on live (Sytox-) $B220^{+}$ Dump- ($CD3^{-}$, $CD11b^{-}$, $Gr1^{-}$) cells and then gated as $CD23^{-}CD21^{-}$ newly formed (NF) B cells, $CD23^{+}CD21^{+}$ follicular (FO) B cells or $CD21^{hi}CD23^{lo}$ marginal zone (MZ) B cells. (**C**) Representative flow cytometry profiles, (**D**) percentage of B cell subsets for each treatment and (**E**) mean absolute number ± SEM of each B cell subset per treatment. (**E**) Each symbol represents an individual mouse. Percent inhibition of treatment compared to vehicle or Ig control is indicated. *$p<0.05$, compared to vehicle control; **$p<0.005$, compared to isotype control; $^{\S}p<0.05$, BR3-Fc compared to 100mg/kg G-744; using two-tailed Student's t-test with Welch's correction.

A

pBtk NZB/W mean (n=5)	IC_{50}	IC_{70}	IC_{90}
G-744 (nM)	475	1206	5465

B

FcεRI/CD63 mean (n=10)	IC_{50}	IC_{70}	IC_{90}
P505-15 (nM)	220	373	669

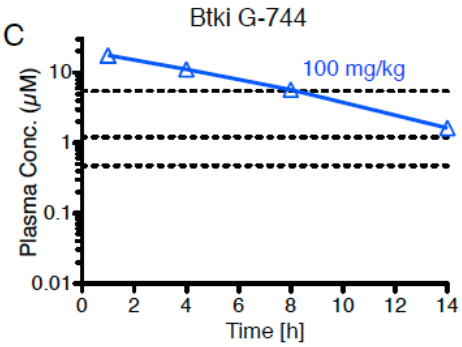

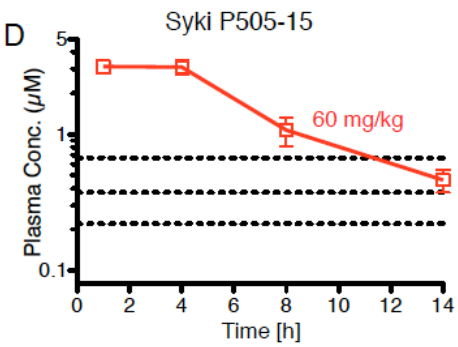

G-744 Dose	% Survival	% Time Above pBTK in 24 hour period		
(mg/kg)		IC_{50}	IC_{70}	IC_{90}
100 BID	100	100	100	67

P505-15 Dose	% Survival	% Time Above FcεRI/ CD63 in 24 hour period		
(mg/kg)		IC_{50}	IC_{70}	IC_{90}
60 BID	70	100	100	92

G-744 Dose	C_{max}	t_{max}	AUC (0-24hr)
(mg/kg)	(μM)	(hr)	(μM*hr)
100 BID	17.6	1	216

P505-15 Dose	C_{max}	t_{max}	AUC (0-24hr)
(mg/kg)	(μM)	(hr)	(μM*hr)
60 BID	3.15	1	47.8

Supplemental Figure 2

In vitro whole blood potency and ex vivo pharmacodynamic readout of Btk and Syk inhibition in NZB/W_F1 whole blood. (**A, B**) Concentration-dependent inhibition of (**A**) anti-IgM F(ab′)$_2$-mediated phosphorylation of Btk-Tyr223 (pBtk) by G-744 in NZB/W_F1 whole blood, (**B**) anti-FcεRI-mediated upregulation of CD63 on basophils by P505-15 in human whole blood. The average potency of 5 (A) or 10 (B) independent experiments is indicated. (**C, D**) Pharmacokinetic profile of (**C**) G-744 and (**D**) P505-15 after oral administration of compound at steady-state. Lines indicate the mean IC_{50}, IC_{70} and IC_{90} concentrations for the inhibition in whole blood of (**C**) Btk-pY223 or (**D**) FcεRI-induced CD63 expression on basophils (pharmacodynamics readout). Time above pharmacodynamics readout and pharmacokinetic profiles for treatment groups is indicated.

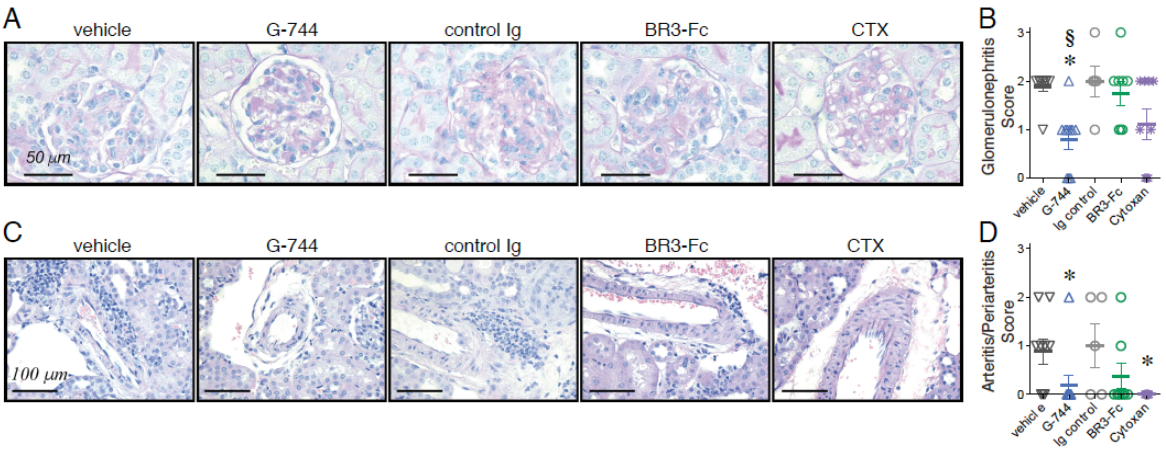

Supplemental Figure 3

Btk inhibition reduces glomerulopathy and arteritis/periarteritis in NZB/W_F1 mice treated with AdIFNα. Fourteen-week old pre-autoimmune NZB/W_F1 female mice (n=10/group) were IFNα-induced and drug-treated for 4 weeks as described in Figure 3. Renal histopathology was examined by immunohistochemistry. (**A**) Glomerulopathy is highlighted by PAS staining of FFPE kidney sections. One representative glomerulus per treatment group is shown in microphotograph. Glomerular involvement is diffuse (>50% of glomeruli affected) and global (entire glomerulus involved). Affected glomeruli typically show hypercellularity and narrowing or obliteration of capillary lumina, the severity of which declines after G-744 or Cyclophosphamide treatment. (**B**) Glomerulopathy scoring. (**C**) Renal arteritis/periarteritis is highlighted by H&E staining of kidney sections. One representative artery per treatment group is shown. (**D**) Periarteritis scoring. (**B, D)** Symbols represent individual mice. Significance indicate *$p<0.05$, G-744 or Cyclophosphamide versus vehicle; $^{§}p<0.05$, compare G-744 with BR3-Fc; using two-tailed Student's t-test with Welch's correction.

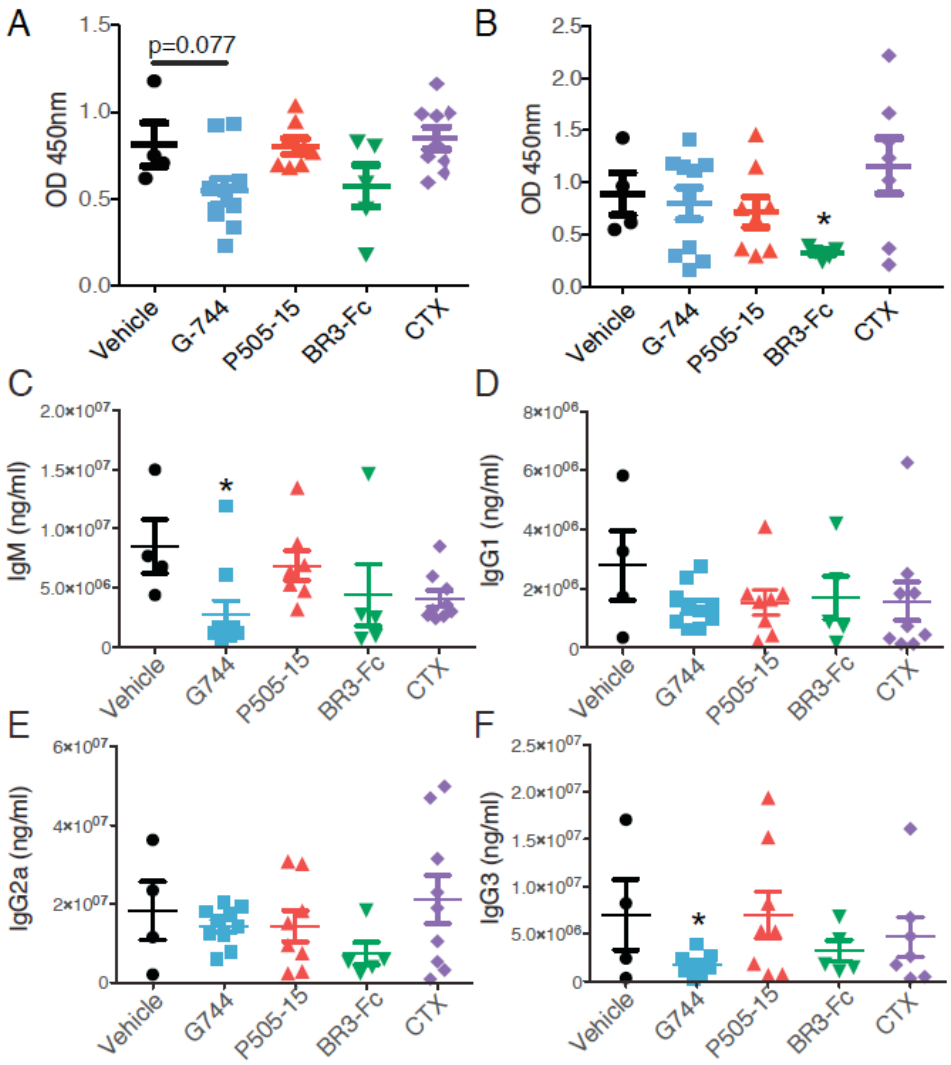

Supplemental Figure 4

Assessment of serum anti-dsDNA antibodies and total Ig titers in the IFNα-enhanced NZB/W_F1 lupus model. Serum samples harvested 7 weeks after treatment start were assessed for (**A, B**) anti-dsDNA and (**C-F**) total Ig titers from the study presented in Fig. 2. (**A**) IgM and (**B**) IgG3 anti-dsDNA Ab titers are presented as optical density (OD) at 450nm where the experimental values were in the linear range of the assay as specified by the ELISA kit manufacturer. Graphs show total (**C**) IgM, (**D**) IgG1, (**E**) IgG2a and (**F**) IgG3 serum concentrations. Statistical differences between treatment and control groups were assessed using Kruskal Wallis test with Dunn's correction, $^{*}p<0.05$. Group means ± SEMs are displayed for each group.

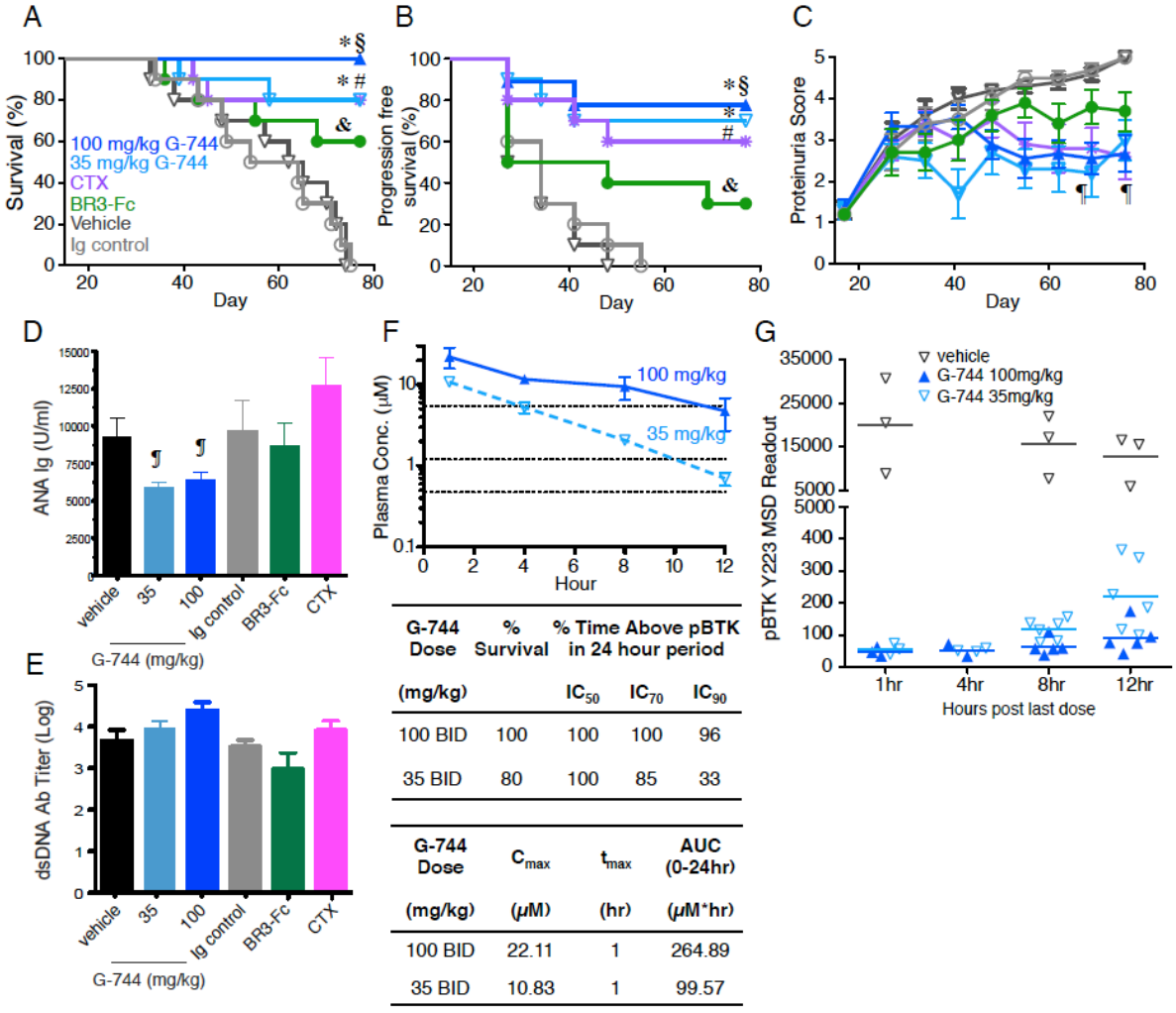

G-744 Dose (mg/kg)	% Survival	% Time Above pBTK in 24 hour period IC_{50}	IC_{70}	IC_{90}
100 BID	100	100	100	96
35 BID	80	100	85	33

G-744 Dose (mg/kg)	C_{max} (μM)	t_{max} (hr)	AUC (0-24hr) (μM*hr)
100 BID	22.11	1	264.89
35 BID	10.83	1	99.57

Supplemental Figure 5

Selective Btk inhibition prolongs survival in IFNα-accelerated NZB/W_F1 mice. Fourteen-week old pre-autoimmune NZB/W_F1 female mice (n=10/group) were administered once adenovirus containing murine IFNα. Drug treatment was started 3 weeks after AdIFNα injection with 100mg/kg G-744 (triangles, dark blue line), 35mg/kg G-744 (open triangles, light blue line), vehicle HPMC (open triangles, black line), 5mg/kg BR3-Fc (circles, green line), Ig control Abs (open circles, grey line) or Cyclophosphamide (stars, magenta line). Graph shows (**A**) percentage of overall survival, (**B**) percentage of progression free survival, and (**C**) proteinuria score as measure of clinical efficacy. (**A, B**) *p<0.001, compare G-744 at 100 mg/kg or 35 mg/kg with vehicle; #p<0.01, compare Cyclophosphamide with vehicle; &p<0.05,

compare BR3-Fc with Ig control; §p<0.05, compare G-774 at 100mg/kg or 35mg/kg with BR3-Fc; (**C**) ¶p<0.05, compare G-744 at 100 mg/kg or 35 mg/kg with vehicle; groups were compared using Log-rank Mantel-Cox test (**A, B**) or Kruskal Wallis test with Dunn's correction (**C**). (**D**) Anti-nuclear antibodies and (**E**) anti-dsDNA autoantibodies were assessed after 6 weeks of drug treatment; significance of the change versus vehicle control was assessed using two-tailed Student's t-test with Welch's correction (¶p< 0.05). (**F, G**) *In vitro* and *ex vivo* pharmacodynamic readout of Btk inhibition in NZB/W_F1 whole blood. (**F**) Pharmacokinetic profile of G-744 after oral administration of compound at steady-state. Lines indicate the mean IC_{50}, IC_{70} and IC_{90} concentrations for the inhibition of pBtk in NZB/W_F1 whole blood (pharmacodynamics readout). Time above pharmacodynamics readout for treatment groups and pharmacokinetic profiles are shown. (**G**) *Ex vivo* analyses of pBtk in whole blood at select pharmacokinetic time points are shown; pBtk levels from vehicle-treated mice were analyzed as reference; symbols represent data from individual mice; the mean for each group is indicated.

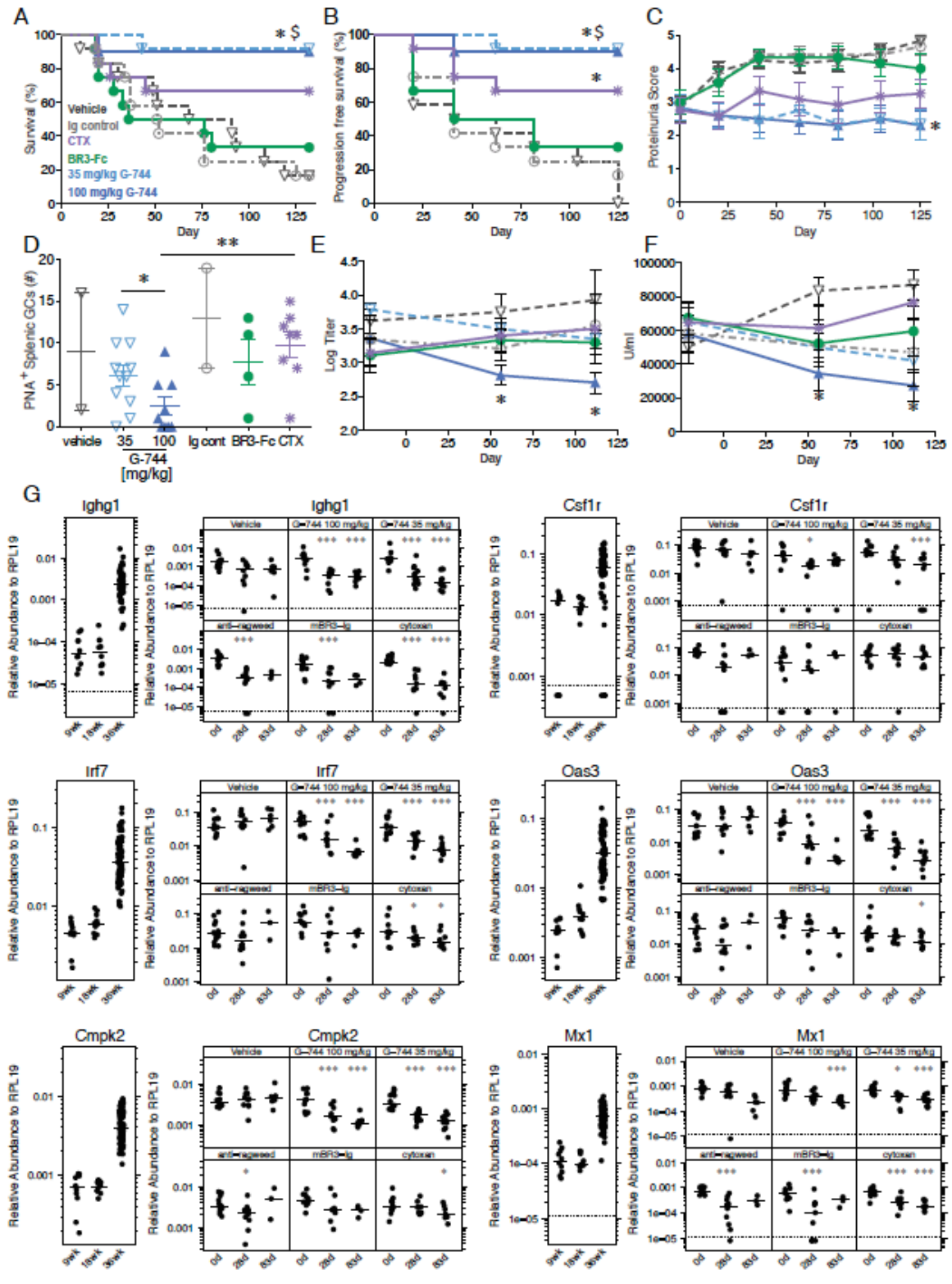

Supplemental Figure 6

Btk inhibition rescues survival in NZB/W_F1 mice with spontaneous disease compared to BR3-Fc. NZB/W_F1 mice (n=12/group) were randomized and treated starting at 36 weeks of age with 100mg/kg G-744 (triangles, dark blue line), 35mg/kg G-744 (open triangles, light blue line), vehicle (open triangles, black line), 5mg/kg BR3-Fc (circles, green line) Ig control Abs (open circles, grey line) or cyclophosphamide (stars, magenta line) as described in Supplemental Material and Methods. Graphs show (**A**) percentage overall survival, (**B**) percentage progression free survival, and (**C**) proteinuria score as measure of clinical efficacy. Statistics is indicated as *$p<0.003$, comparison of G-744 at 100 mg/kg or 35 mg/kg with vehicle. $^{\S}p<0.03$, comparison of G-744 at 100mg/kg or 35mg/kg with BR3-Fc. Groups were compared using Log-rank Mantel-Cox test. (**D**) The number of PNA+ GCs was evaluated from FFPE spleens of surviving mice after 134 days of treatment by immunohistochemistry. Group means and SEMs were calculated for each group, the 100mg/kg G-744-treated group was compared to other groups using 2-tailed heteroscedastic Student's t-tests; *$p<0.05$; **$p<0.005$. A statistical comparison to vehicle control was not meaningful as only 2 vehicle-treated mice survived at the end of the study. (**E, F**) Anti-dsDNA (**E**) and anti-histone (**F**) autoantibodies were assessed by ELISA; *$p<0.05$ using one-way Dunnett's test at day56 and day112. (**G**) Expression of IFNα-regulated genes after drug treatment for 28 or 83 days were determined by quantitative RT-PCR (fluidigm) from RNA isolated from whole blood of surviving mice. Baseline levels of genes (for genes included in analyses see Supplemental Table 2) were determined at mouse ages of 9, 18 and 36 weeks (= d-5 before drug treatment start). Values are the relative expression of each gene to the control gene, RPL19. Dotted lines represent the lower limit of detection. Although the spontaneous NZB/W_F1 model is only associated with mild induction of type-I IFNs, particularly early during disease progression, gene expression analysis from whole blood demonstrated that expression of several IFN-regulated genes increased at 36 weeks of age around the time when severe renal disease manifests and mice start to succumb to lupus disease. *$p<0.05$, **$p<0.005$, ***$p<0.0005$ versus 36-week old untreated mice using linear regression as described above.

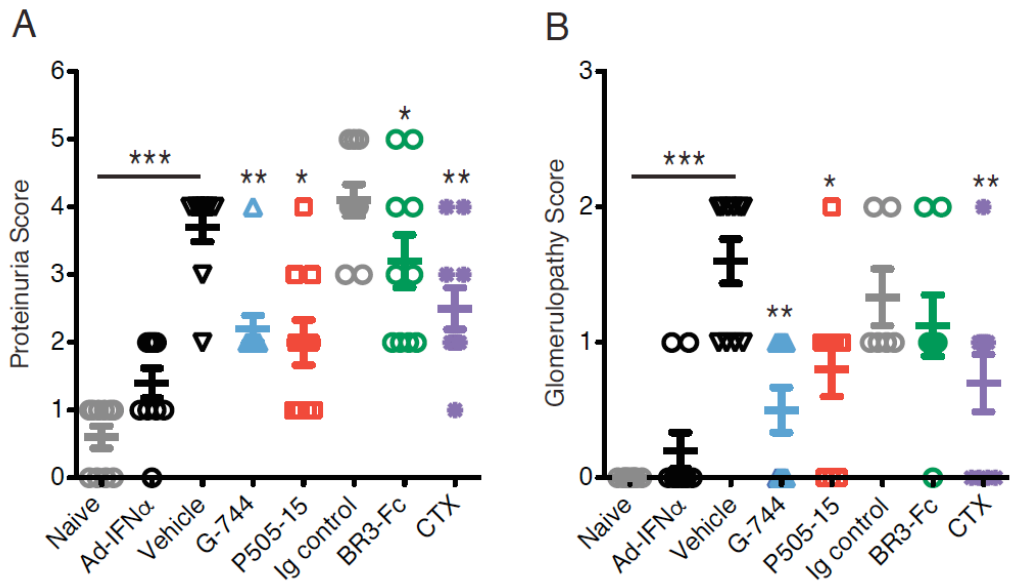

Supplemental Figure 7

Proteinuria and glomerulopathy scores after short-term treatment with G-744, P505-15 or cyclophosphamide in IFNα-accelerated LN in NZB/W_F1 mice. (**A**) Proteinuria scores and (**B**) Glomerulopathy scoring after 4-week drug treatment in IFNα-accelerated NZB/W_F1 mice from the experiment described in Figure 4 versus naïve and AdIFNα-treated NZB/W_F1 control groups. Naïve group animals were 17-week old NZB/W_F1 animals that were not injected with AdIFNα and showed no (20%), trace (20%) or 30mg/dl (60%) proteinuria at time of measurement. AdIFNα group animals were 17-week old NZB/W_F1 animals that were injected with AdIFNα for 3 weeks and showed trace (10%), 30mg/dl (40%) or 100mg/dl (50%) proteinuria. Protenuria was assessed on day 20 after AdIFNα treatment start, one day before drug treatment start on day 21. *p<0.05, **p<0.005, calculated using the Student's t-test with Welch's correction.

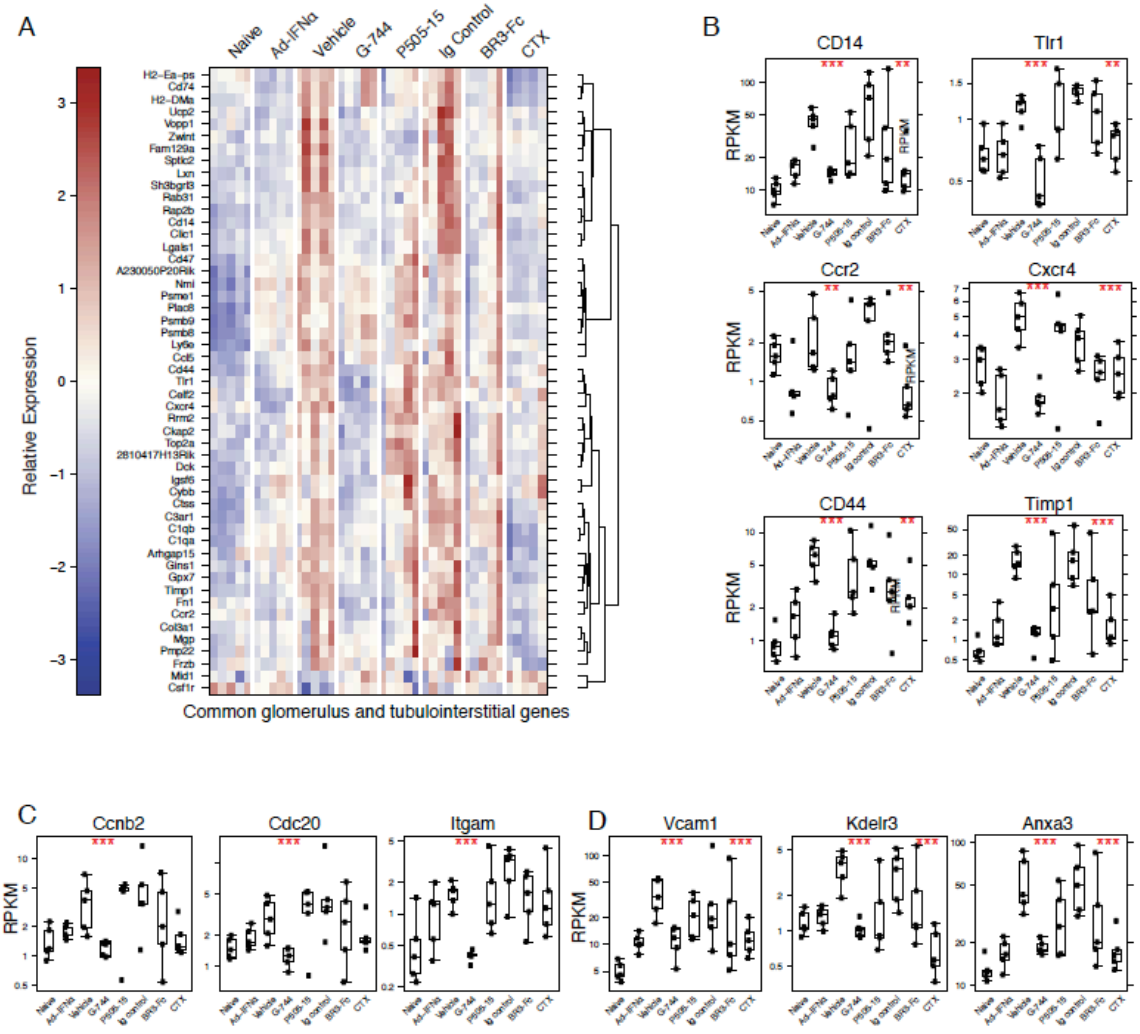

Supplemental Figure 8

Gene expression changes in kidney after cytoxan treatment or blockade of Btk, Syk, or BAFF in IFNα-precipitated LN in NZB/W_F1 mice. RNA sequencing analysis was performed on kidney RNA derived from the experiment described in Figure 6. (**A**) Effect of drug treatment on human LN ortholog genes previously identified to be commonly up-regulated in both the glomerulus and tubulointerstitium of nephritic kidneys from human LN patients (see Methods for details). Genes that showed individual significant changes with any treatment versus their respective controls are indicated (≥1.5-fold difference between groups with an adjusted p-value <0.01). Each column in the heatmap represents one animal within each treatment group. (**B-D**) Boxplot of 'Reads Per Kilobase of transcript per Million mapped reads'

(RPKM) expression of select individual genes from (**B**) common glomerulus and tubulointerstitial genes shown in (A), (**C**) glomerulus genes shown in Fig. 6a, and (**C**) tubulointerstitial genes shown in Fig. 6b. Gene expression data were plotted using boxplots overlaid with all observed data points. The box corresponds to the 1st quartile, median (black line), and 3rd quartile. The whiskers extend to the most extreme data point that is no more than 1.5-times the interquartile range from the box; *$p<0.05$, **$p<0.005$, ***$p<0.0005$, using DESeq2 to fit a negative binomial model, as described above.

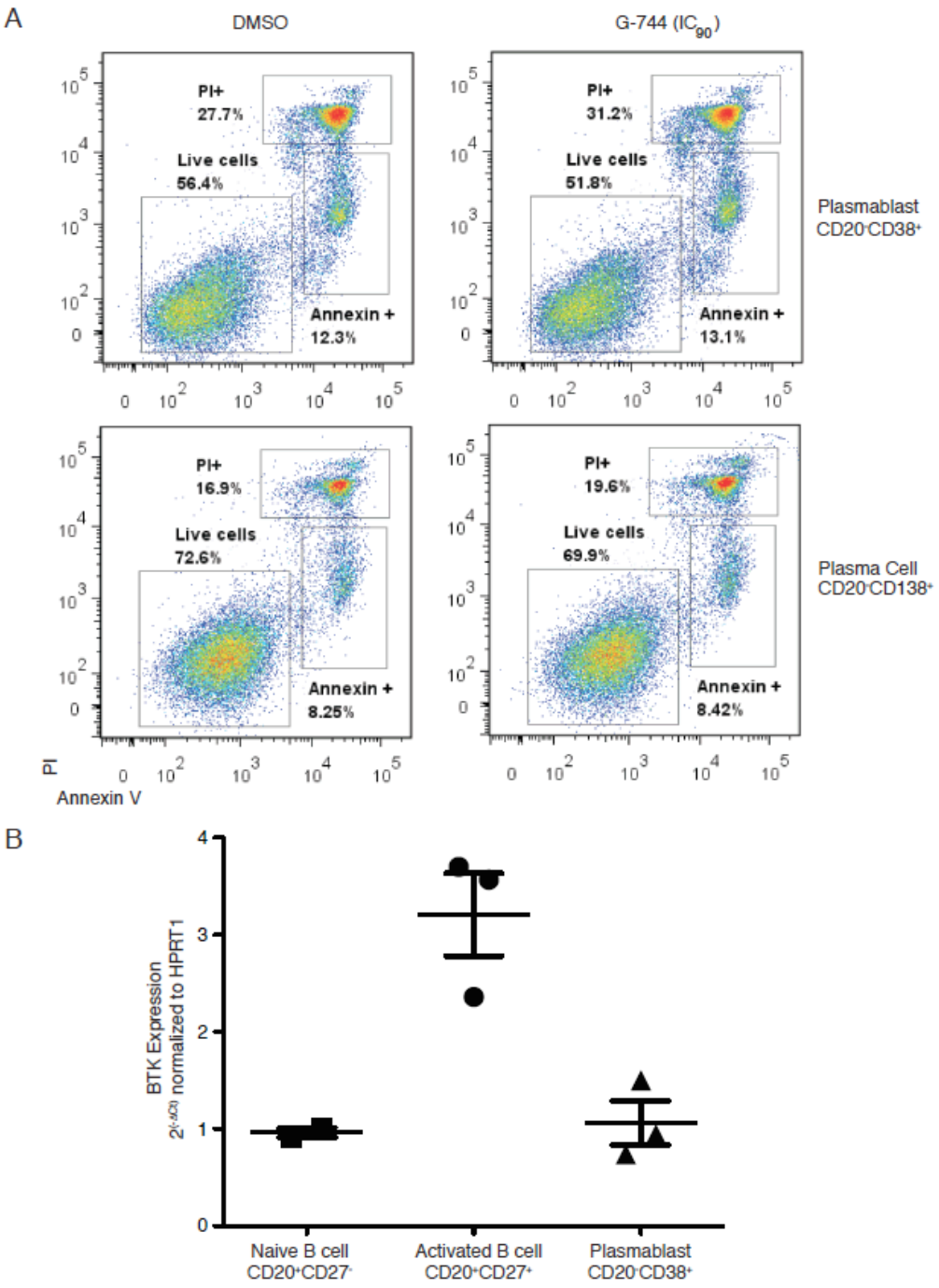

Supplemental Figure 9

Assessment of plasmablast/plasma cell survival in presence of G-744 and of Btk RNA expression in B cell lineage populations. (**A**) Plasmablasts and plasma cells were differentiated from memory B cells ($CD20^+CD27^+$) under culture conditions containing TLR stimulation and cytokines as described in the Supplemental Methods.

After 14 days, plasmablasts ($CD20^{-}CD38^{+}$) and plasma cells ($CD20^{-}CD138^{+}$) were sorted by flow cytometry and placed in culture with vehicle (DMSO) or G-744 at the IC_{90} inhibition concentration (650 nM) for 2 days. Cells were then assessed for viability using Annexin V and Propidium Iodide (PI) staining. (**B**) Btk RNA expression in naïve B cells ($CD20^{+}CD27^{-}$), activated B cells ($CD20^{+}CD27^{+}$) and plasmablasts ($CD20^{lo}CD38^{+}$) as indicated (n=3 for each lineage); naïve B cells were sorted from human peripheral blood mononuclear cells, plasmablasts were differentiated as in (A) and purified by flow cytomtery, and activated B cells were also sorted from the plasmablast differentiation cultures; Btk transcript levels were examined by quantitative RT-PCR; data are shown as relative abundance of Btk transcript normalized to HPRT.

Supplemental References

1. Perry D, Sang A, Yin Y, Zheng YY, and Morel L. Murine models of systemic lupus erythematosus. *Journal of Biomedicine & Biotechnology.* 2011;2011(271694.
2. Wu TD, and Nacu S. Fast and SNP-tolerant detection of complex variants and splicing in short reads. *Bioinformatics.* 2010;26(7):873-81.
3. Honigberg LA, Smith AM, Sirisawad M, Verner E, Loury D, Chang B, Li S, Pan Z, Thamm DH, Miller RA, et al. The Bruton tyrosine kinase inhibitor PCI-32765 blocks B-cell activation and is efficacious in models of autoimmune disease and B-cell malignancy. *Proceedings of the National Academy of Sciences of the United States of America.* 2010;107(29):13075-80.
4. Xu D, Kim Y, Postelnek J, Vu MD, Hu DQ, Liao C, Bradshaw M, Hsu J, Zhang J, Pashine A, et al. RN486, a selective Bruton's tyrosine kinase inhibitor, abrogates immune hypersensitivity responses and arthritis in rodents. *The Journal of Pharmacology and Experimental Therapeutics.* 2012;341(1):90-103.
5. Coffey G, DeGuzman F, Inagaki M, Pak Y, Delaney SM, Ives D, Betz A, Jia ZJ, Pandey A, Baker D, et al. Specific inhibition of spleen tyrosine kinase suppresses leukocyte immune function and inflammation in animal models of rheumatoid arthritis. *The Journal of Pharmacology and Experimental Therapeutics.* 2012;340(2):350-9.
6. Rankin AL, Seth N, Keegan S, Andreyeva T, Cook TA, Edmonds J, Mathialagan N, Benson MJ, Syed J, Zhan Y, et al. Selective inhibition of BTK prevents murine lupus and antibody-mediated glomerulonephritis. *J Immunol.* 2013;191(9):4540-50.